

†Electronic supplementary information (ESI)

Ancillary ligand induced variation in electronic spectral and catalytic properties of heteroleptic ONO-pincer complexes of ruthenium†

Papu Dhibar,^{a,b,§} Anushri Chandra,^{a,§} Piyali Paul^c and Samaresh Bhattacharya^{*a}

^a *Department of Chemistry, Inorganic Chemistry Section, Jadavpur University, Kolkata - 700 032, India. E-mail: samareshb.chemistry@jadavpuruniversity.in*

^b *Department of Chemistry, Brainware University, Kolkata 700 125, India*

^c *Department of Chemistry and Environment, Heritage Institute of Technology, Kolkata-700 107, India*

§ Equal contribution.

Contents:

Fig. S1	ORTEP diagram showing the crystal structure of 1	Pg. 3
Fig. S2	ORTEP diagram showing the crystal structure of 2	Pg. 3
Fig. S3	ORTEP diagram showing the crystal structure of 3	Pg. 4
Fig. S4	ORTEP diagram showing the crystal structure of 4	Pg. 4
Table S1	Selected bond distances and bond angles for 1	Pg. 5
Table S2	Selected bond distances and bond angles for 2	Pg. 5
Table S3	Selected bond distances and bond angles for 3	Pg. 6
Table S4	Selected bond distances and bond angles for 4	Pg. 6
Fig. S5	Intermolecular C-H \cdots O=C, C-H \cdots C and C \cdots O=C interactions in the lattice of complex 1	Pg. 7
Fig. S6	Intermolecular C-H \cdots O=C, C-H \cdots C, C-H \cdots O-C and C \cdots O=C interactions in the lattice of complex 3	Pg. 7
Fig. S7-S9	^1H , ^{13}C , ^{31}P NMR spectra of 1	Pg. 8-9
Fig. S10-S12	^1H , ^{13}C , ^{31}P NMR spectra of 2	Pg. 9-10
Fig. S13-S15	^1H , ^{13}C , ^{31}P NMR spectra of 3	Pg. 11-12
Fig. S16-S18	^1H , ^{13}C , ^{31}P NMR spectra of 4	Pg. 12-13
Fig. S19	ESI-MS spectrum of 1	Pg. 14
Fig. S20	ESI-MS spectrum of 2	Pg. 14
Fig. S21	ESI-MS spectrum of 3	Pg. 15
Fig. S22	ESI-MS spectrum of 4	Pg. 15
Table S5-S12	Computed parameters from TDDFT calculations on 1 , 2 , 3 and 4 for electronic spectral properties & compositions of selected molecular orbitals associated with the electronic spectral transitions	Pg. 16-29
Fig. S23-S26	Contour plots of the molecular orbitals associated with the electronic spectral transitions.	
Table S13	Optimization of the reaction conditions for the catalysis	Pg. 30
Table S14	Comparison of efficiency of different Ru-catalysts for the transfer hydrogenation	Pg. 31
Table S15	Crystallographic data for 1 , 2 , 3 and 4	Pg. 32

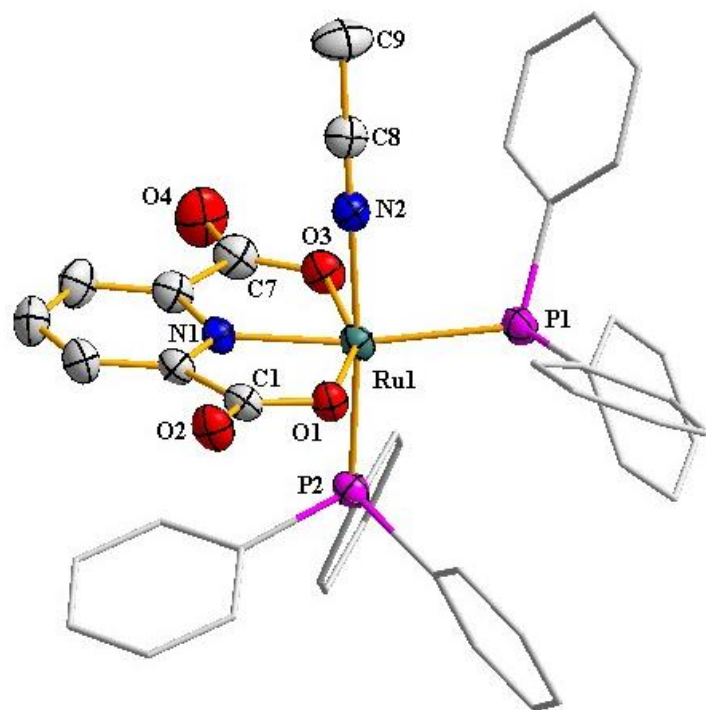


Fig. S1 ORTEP diagram showing the crystal structure of **1** (The ellipsoids are drawn at the 40% probability level).

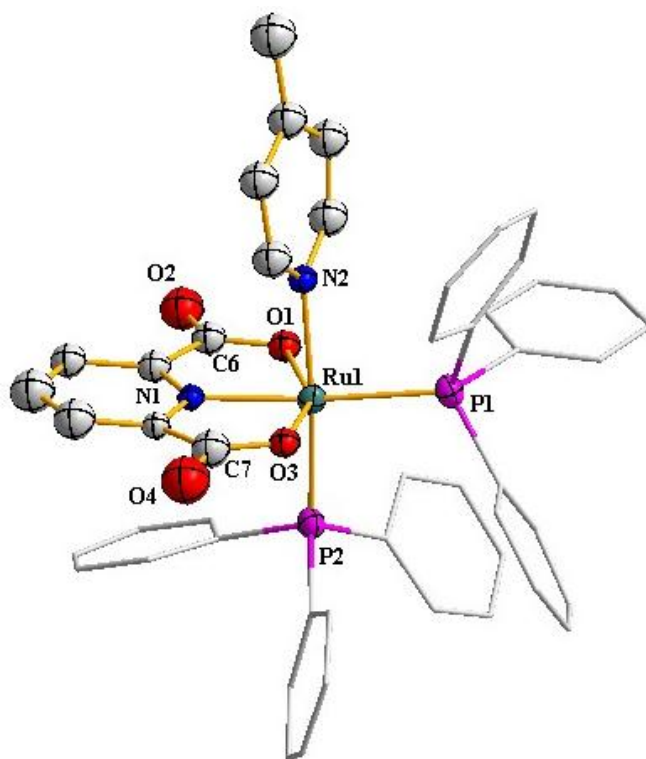


Fig. S2 ORTEP diagram showing the crystal structure of **2** (The ellipsoids are drawn at the 40% probability level).

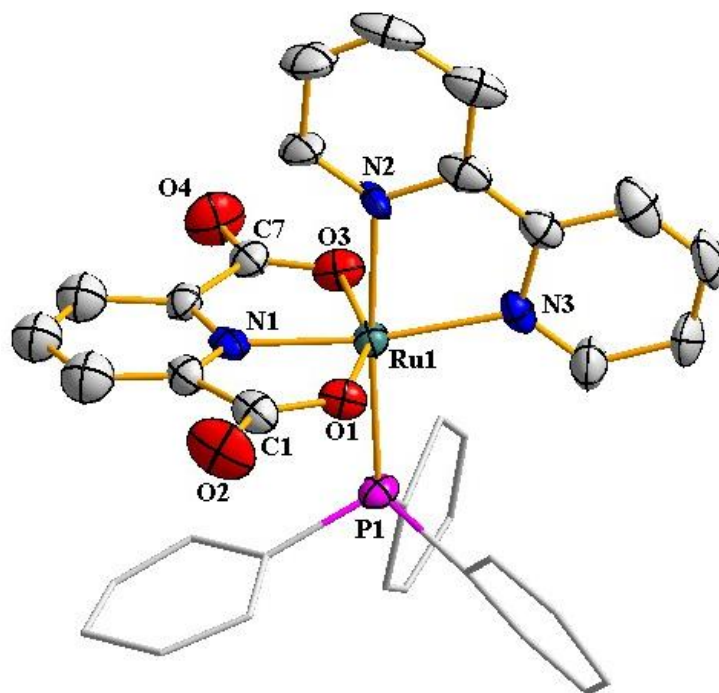


Fig. S3 ORTEP diagram showing the crystal structure of **3** (The ellipsoids are drawn at the 40% probability level).

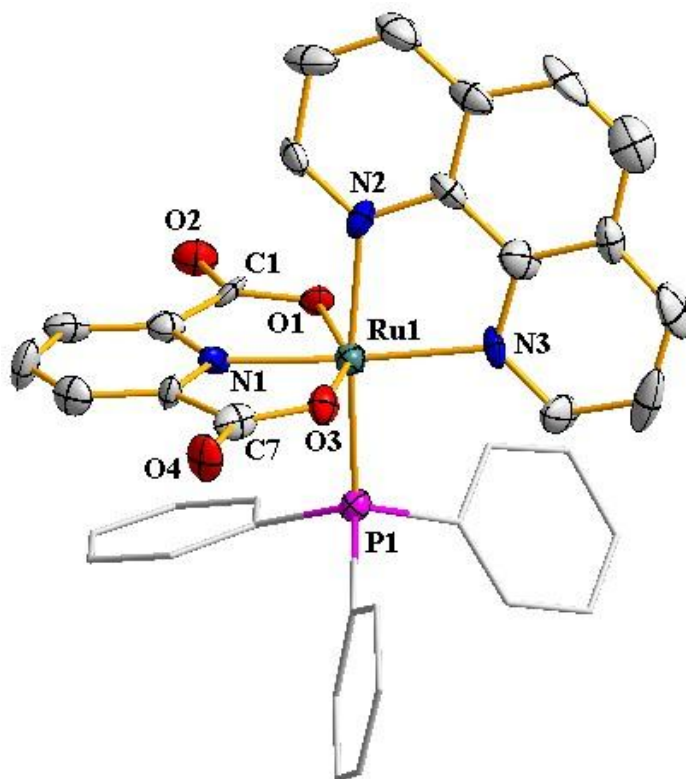


Fig. S4 ORTEP diagram showing the crystal structure of **4** (The ellipsoids are drawn at the 50% probability level).

Table S1 Selected bond distances and bond angles of **1**

Bond distances (Å)			
Ru1-N1	2.0038(15)	C1-O1	1.291(2)
Ru1-N2	2.0949(17)	C1-O2	1.226(2)
Ru1-O1	2.1394(13)	C7-O3	1.294(3)
Ru1-O3	2.1261(13)	C7-O4	1.220(3)
Ru1-P1	2.3462(5)	C8-N2	1.132(3)
Ru1-P2	2.3133(5)	C8-C9	1.452(3)
Bond angles (°)			
N1-Ru1-P1	170.72(5)	N1-Ru1-O1	77.55(5)
N2-Ru1-P2	174.94(5)	N1-Ru1-O3	78.17(6)
O1-Ru1-O3	155.43(5)	Ru1-N2-C8	172.71(16)
N1-Ru1-N2	83.42(6)	N2-C8-C9	177.0(2)

Table S2 Selected bond distances and bond angles for **2**

Bond distances (Å)			
Ru1-N1	2.000(4)	Ru1-P2	2.3255(14)
Ru1-N2	2.160(4)	C6-O1	1.282(6)
Ru1-O1	2.114(3)	C6-O2	1.235(7)
Ru1-O3	2.144(3)	C7-O3	1.300(6)
Ru1-P1	2.3374(15)	C7-O4	1.219(6)
Bond angles (°)			
N1-Ru1-P1	171.59(12)	N1-Ru1-O1	78.20(15)
N2-Ru1-P2	171.61(12)	N1-Ru1-O3	77.68(15)
O1-Ru1-O3	155.61(14)	N1-Ru1-N2	84.29(15)

Table S3 Selected bond distances and bond angles for **3**

Bond distances (Å)			
Ru1-N1	1.98(5)	Ru1-P1	2.35(5)
Ru1-N2	2.11(4)	C1-O1	1.29(3)
Ru1-N3	2.10(5)	C1-O2	1.22(2)
Ru1-O1	2.15(4)	C7-O3	1.29(4)
Ru1-O3	2.13(4)	C7-O4	1.24(2)
Bond angles (°)			
N1-Ru1-N3	170.4(4)	N1-Ru1-O1	78.3(5)
N2-Ru1-P1	172.7(3)	N1-Ru1-O3	78.9(12)
O1-Ru1-O3	156.7(7)	N2-Ru1-N3	78.0(6)

Table S4 Selected bond distances and bond angles for **4**

Bond distances (Å)			
Ru1-N1	1.982(12)	Ru1-P1	2.312(45)
Ru1-N2	2.125(11)	C1-O1	1.287(17)
Ru1-N3	2.111(12)	C1-O2	1.217(16)
Ru1-O1	2.200(10)	C7-O3	1.336(17)
Ru1-O3	2.109(10)	C7-O4	1.179(17)
Bond angles (°)			
N1-Ru1-N3	167.9(5)	N1-Ru1-O1	77.6(4)
N2-Ru1-P1	170.2 (3)	N1-Ru1-O3	78.7(4)
O1-Ru1-O3	155.9 (4)	N2-Ru1-N3	78.1(4)

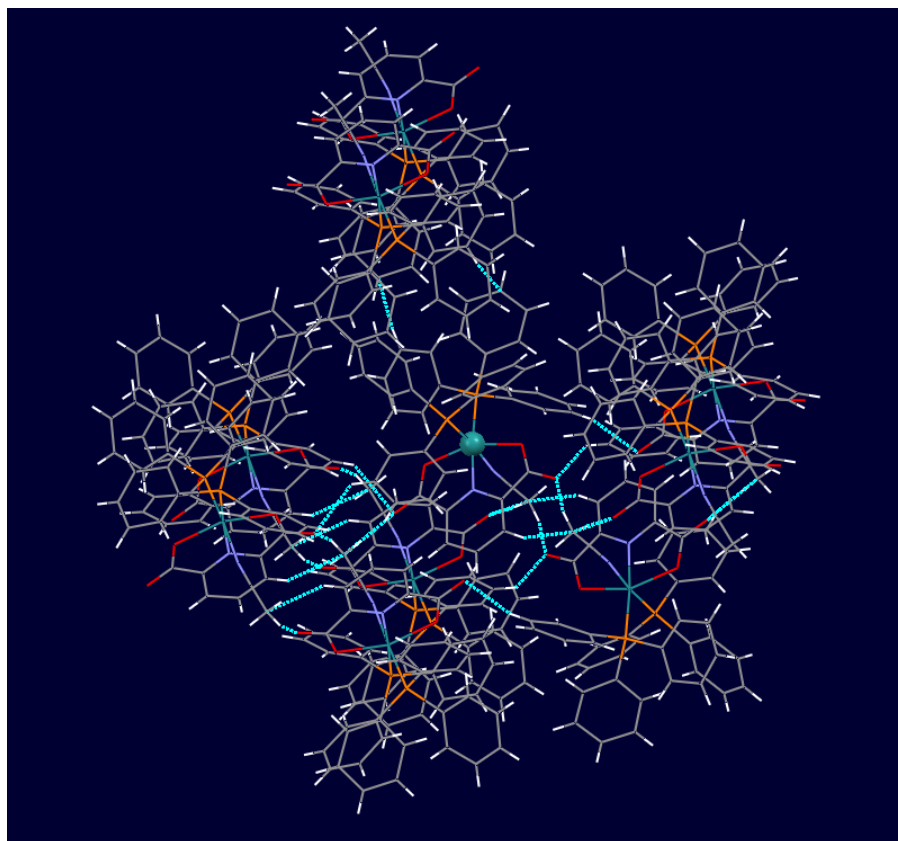


Fig. S5 Intermolecular C-H...O=C, C-H...C and C...O=C interactions in the lattice of complex **1**.

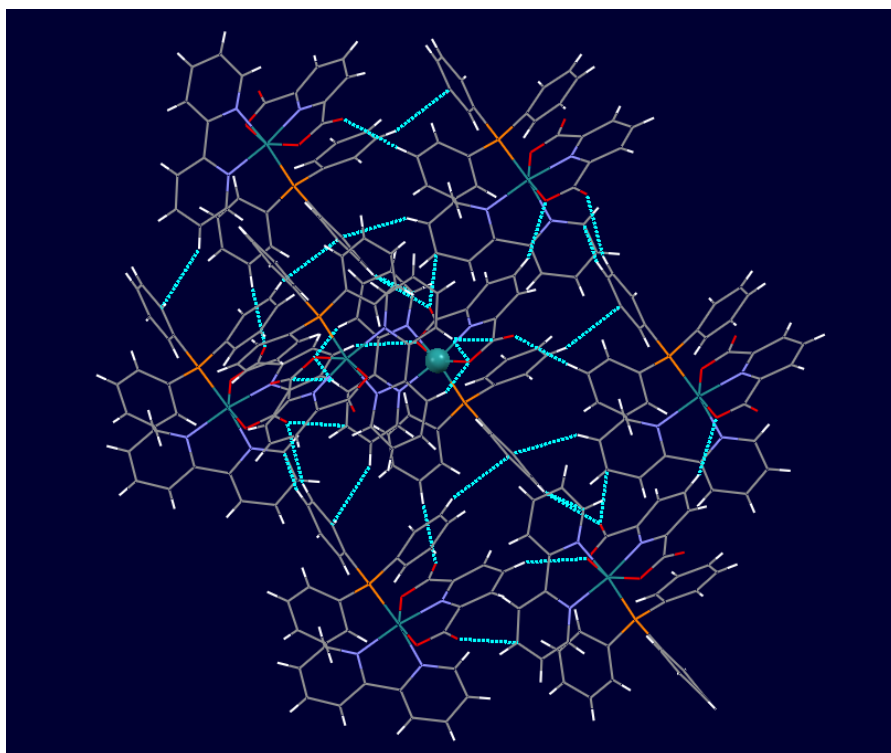


Fig. S6 Intermolecular C-H...O=C, C-H...C, C-H...O-C and C...O=C interactions in the lattice of complex **3**.

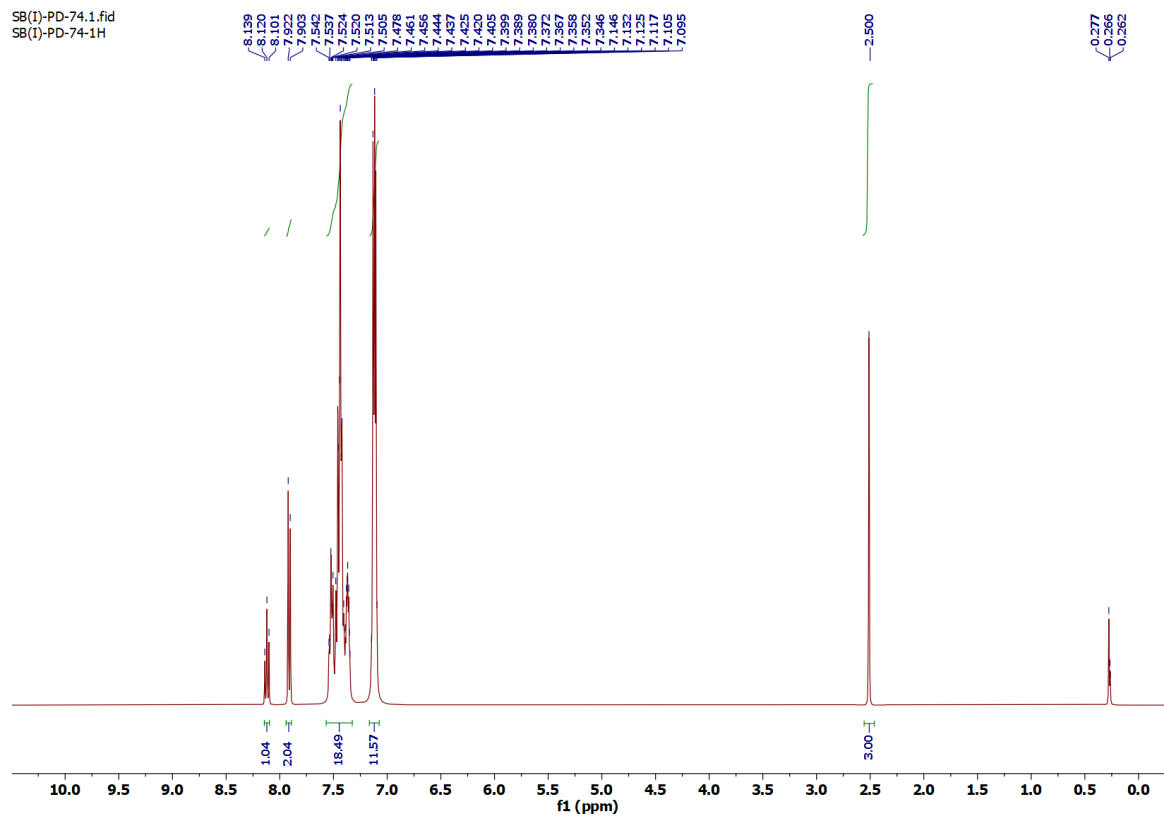


Fig. S7 ^1H NMR spectrum of **1** in CD_3OD solution.

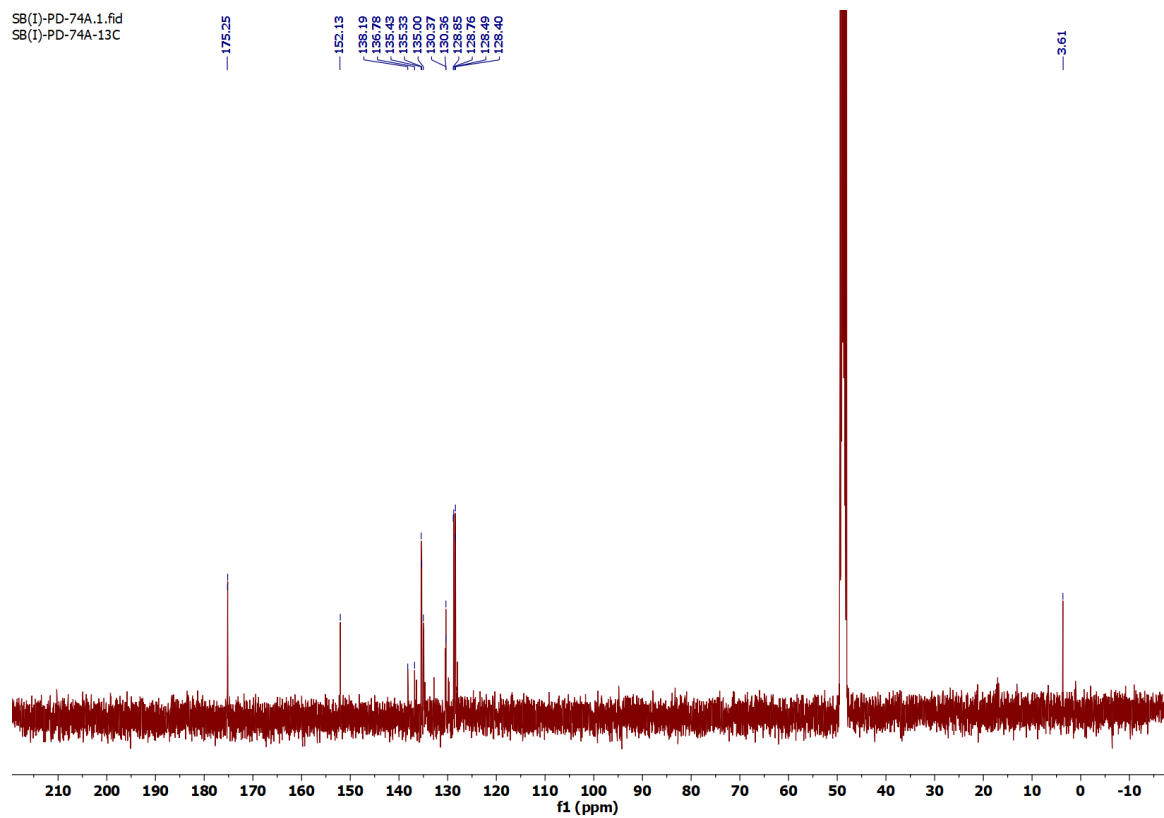


Fig. S8 $^{13}\text{C}\{^1\text{H}\}$ NMR spectrum of **1** in CD_3OD solution.

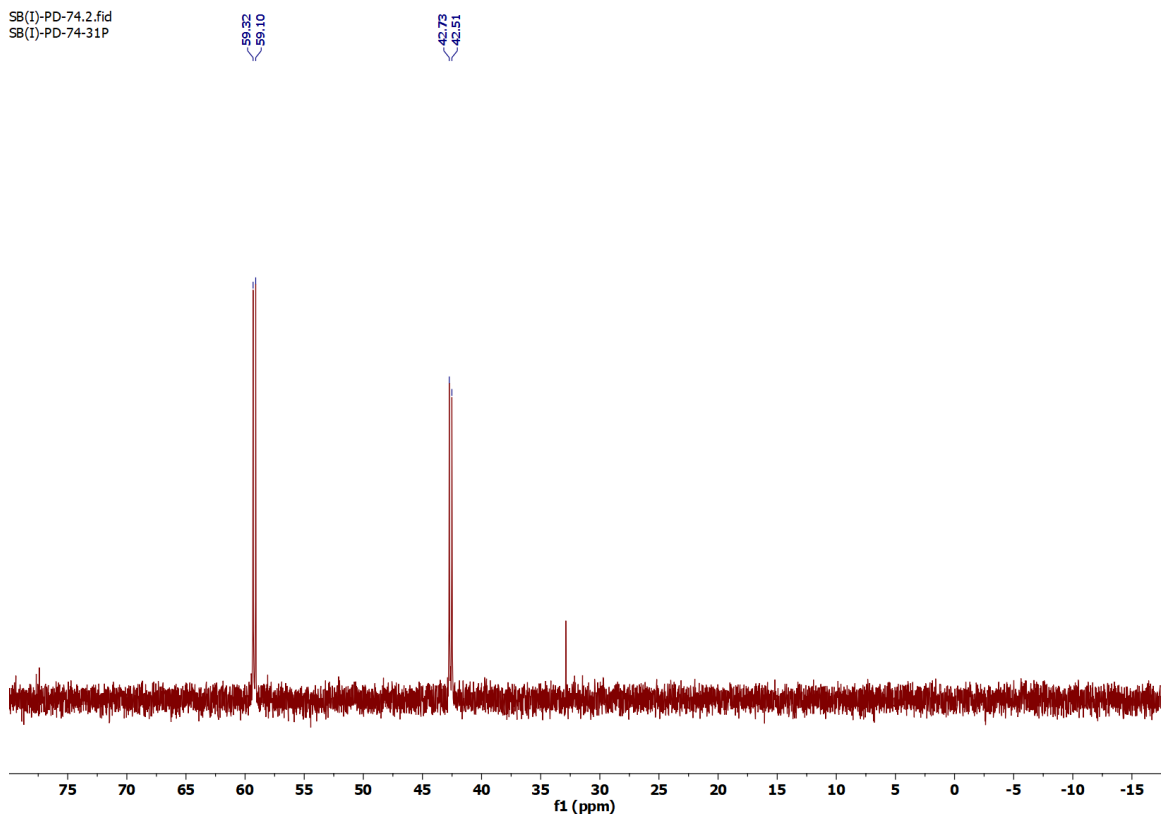


Fig. S9 $^{31}\text{P}\{^1\text{H}\}$ NMR spectrum of **1** in CD_3OD solution.

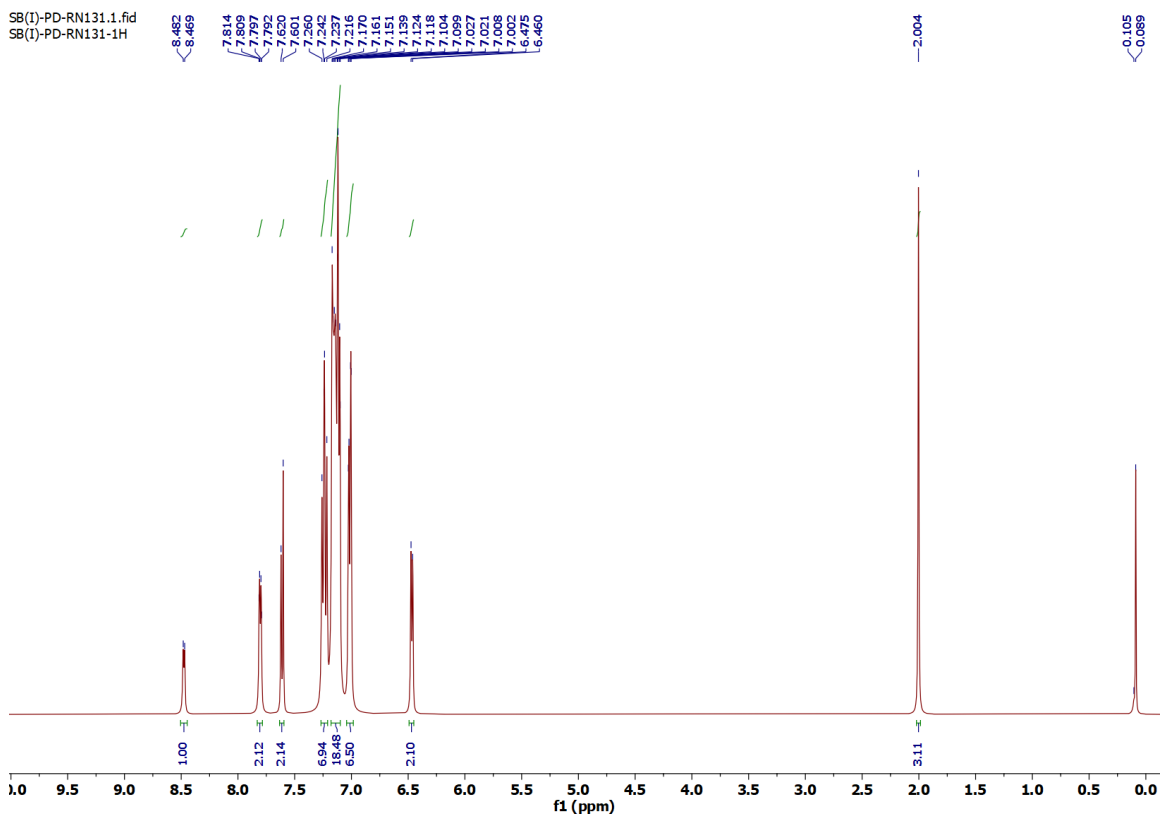


Fig. S10 ^1H NMR spectrum of **2** in CDCl_3 solution.

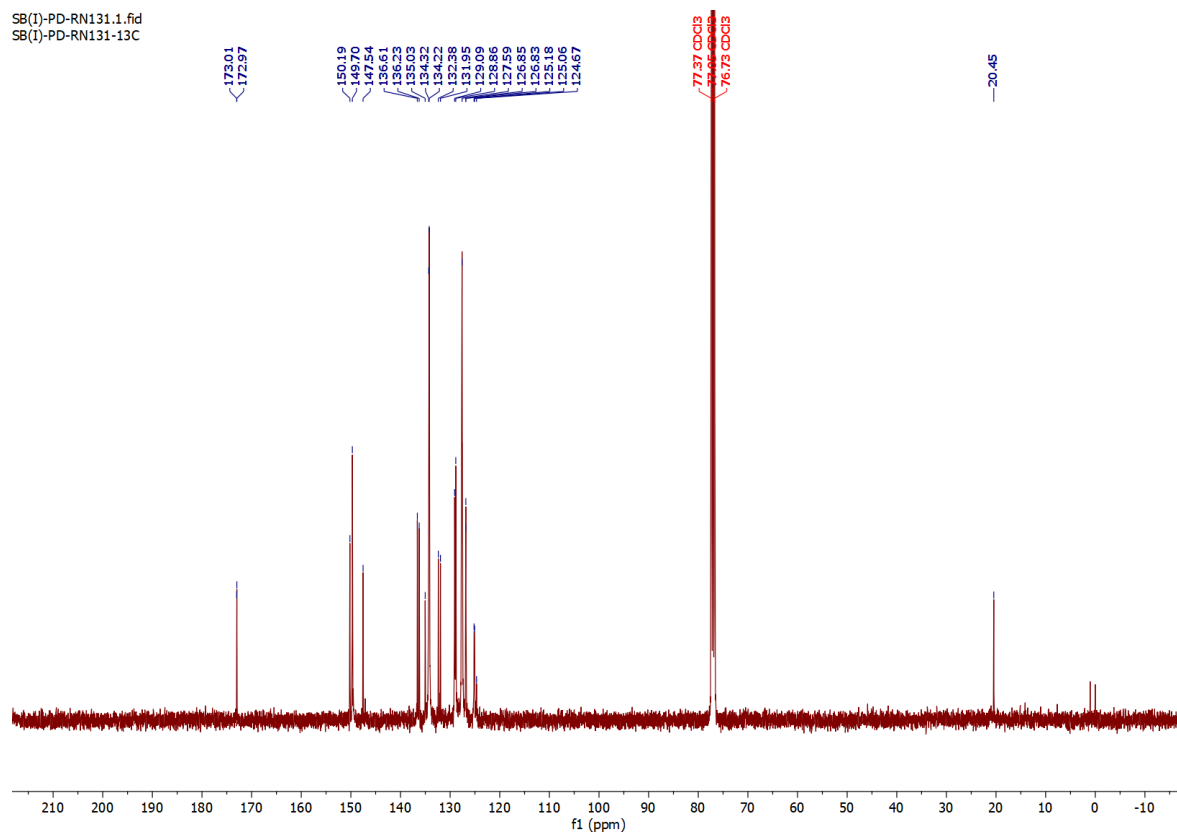


Fig. S11 $^{13}\text{C}\{^1\text{H}\}$ NMR spectrum of **2** in CDCl_3 solution.

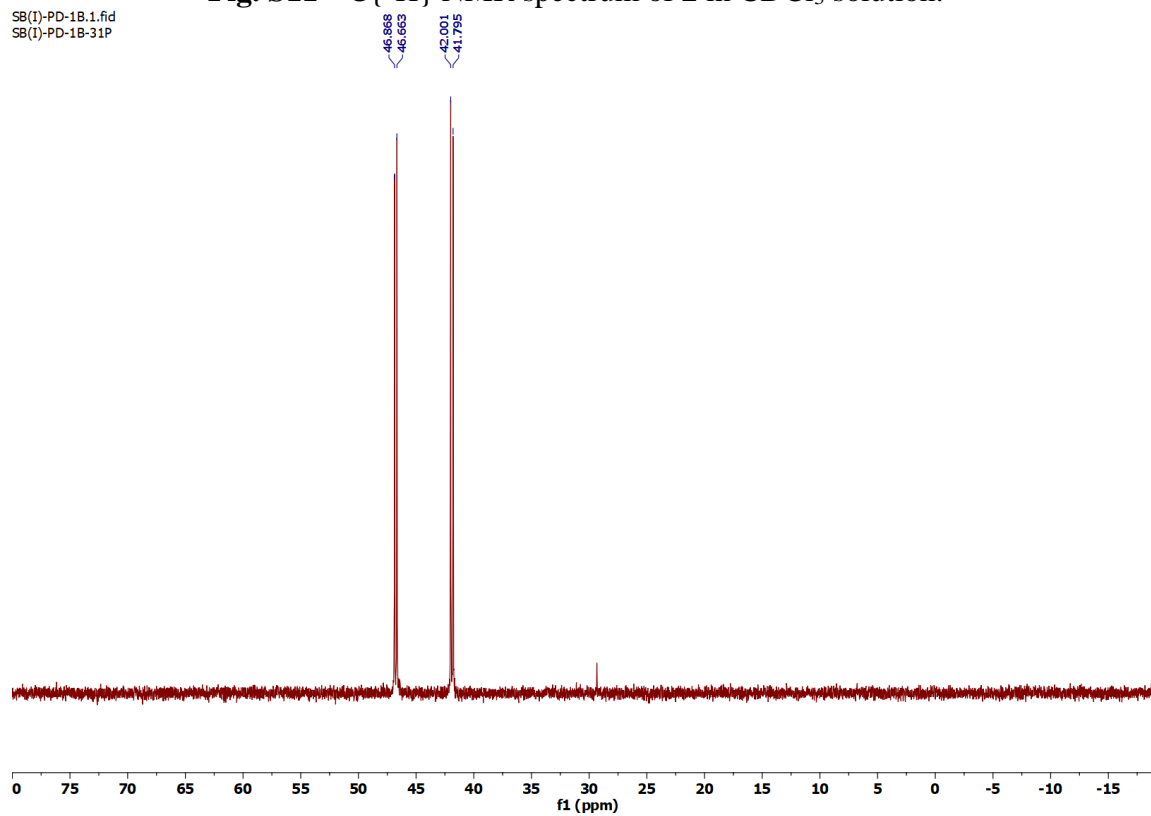


Fig. S12 $^{31}\text{P}\{^1\text{H}\}$ NMR spectrum of **2** in CDCl_3 solution.

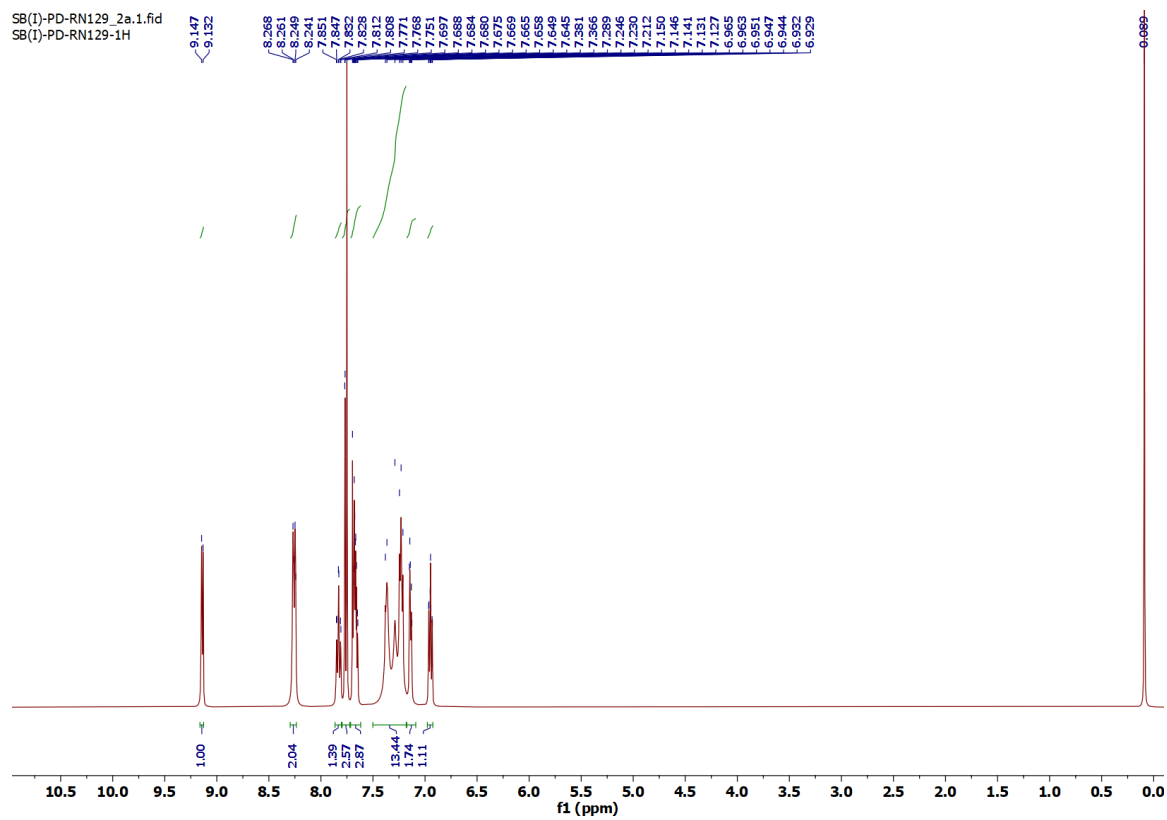


Fig. S13 ^1H NMR spectrum of **3** in CDCl_3 solution.

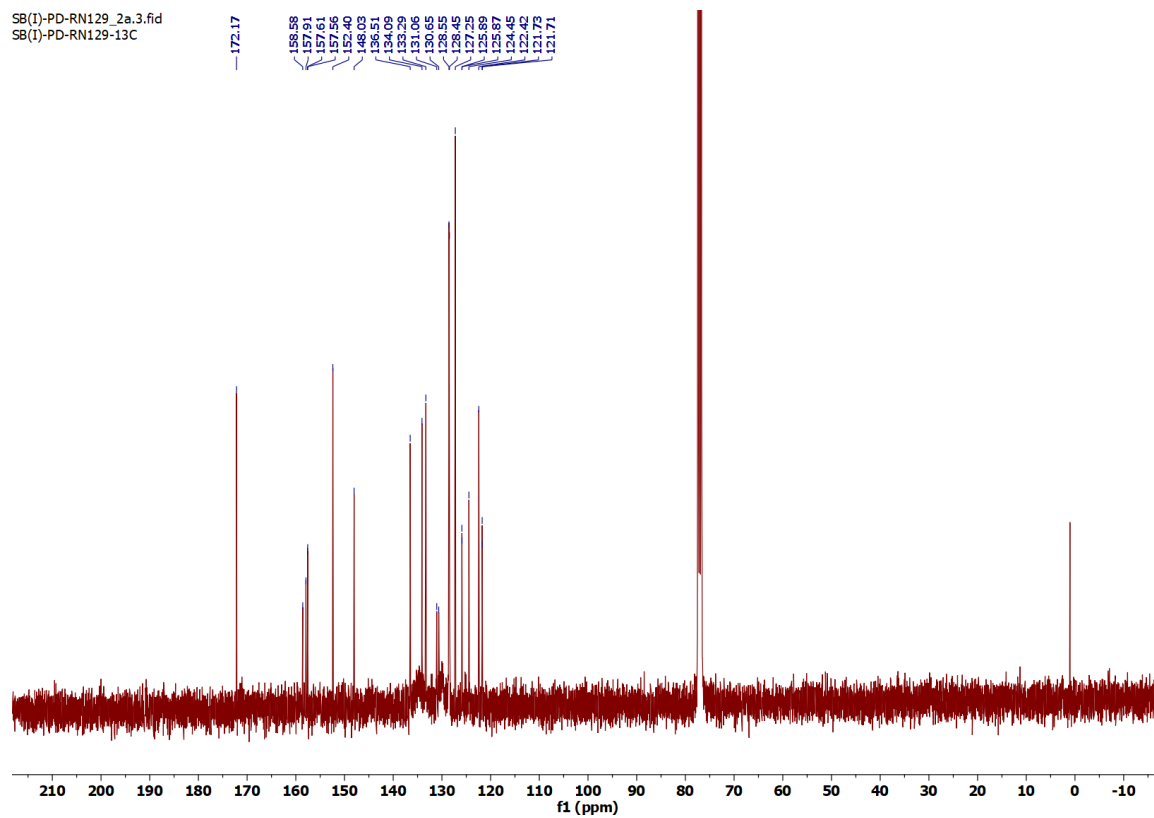


Fig. S14 $^{13}\text{C}\{^1\text{H}\}$ NMR spectrum of **3** in CDCl_3 solution.

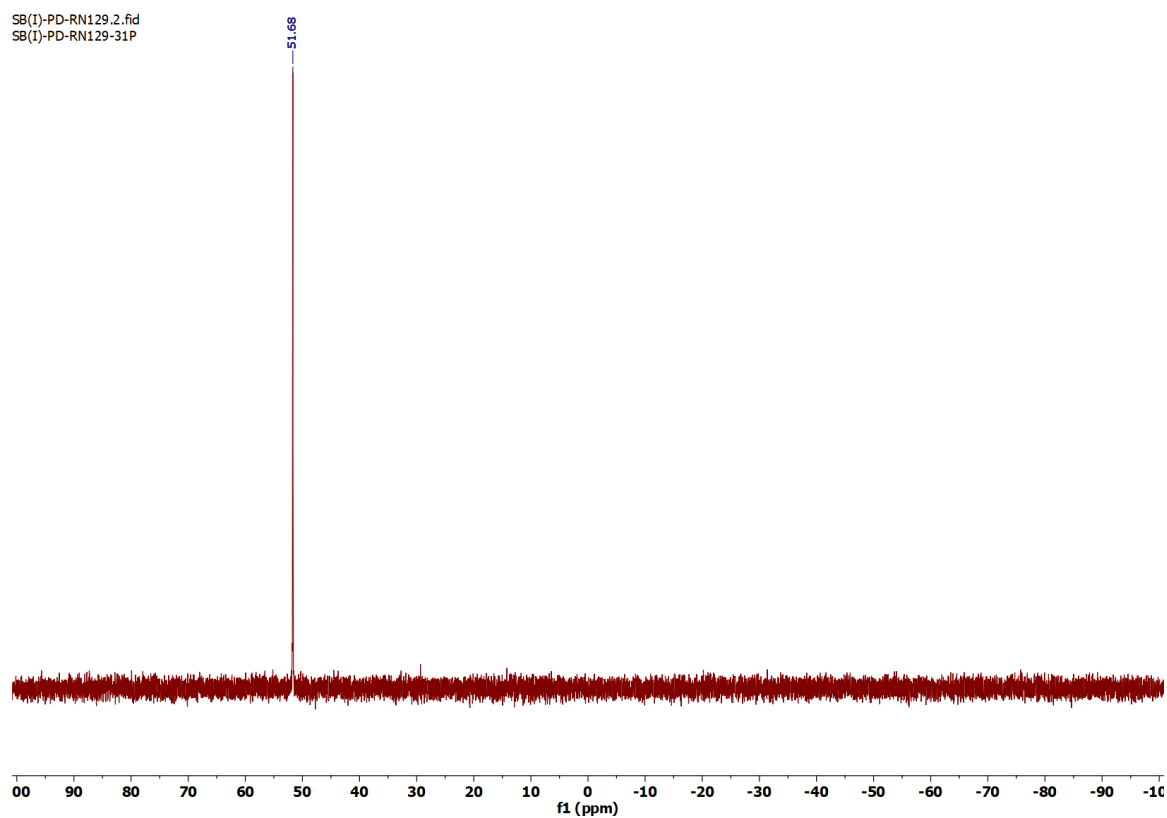


Fig. S15 $^{31}\text{P}\{^1\text{H}\}$ NMR spectrum of **3** in CDCl_3 solution.

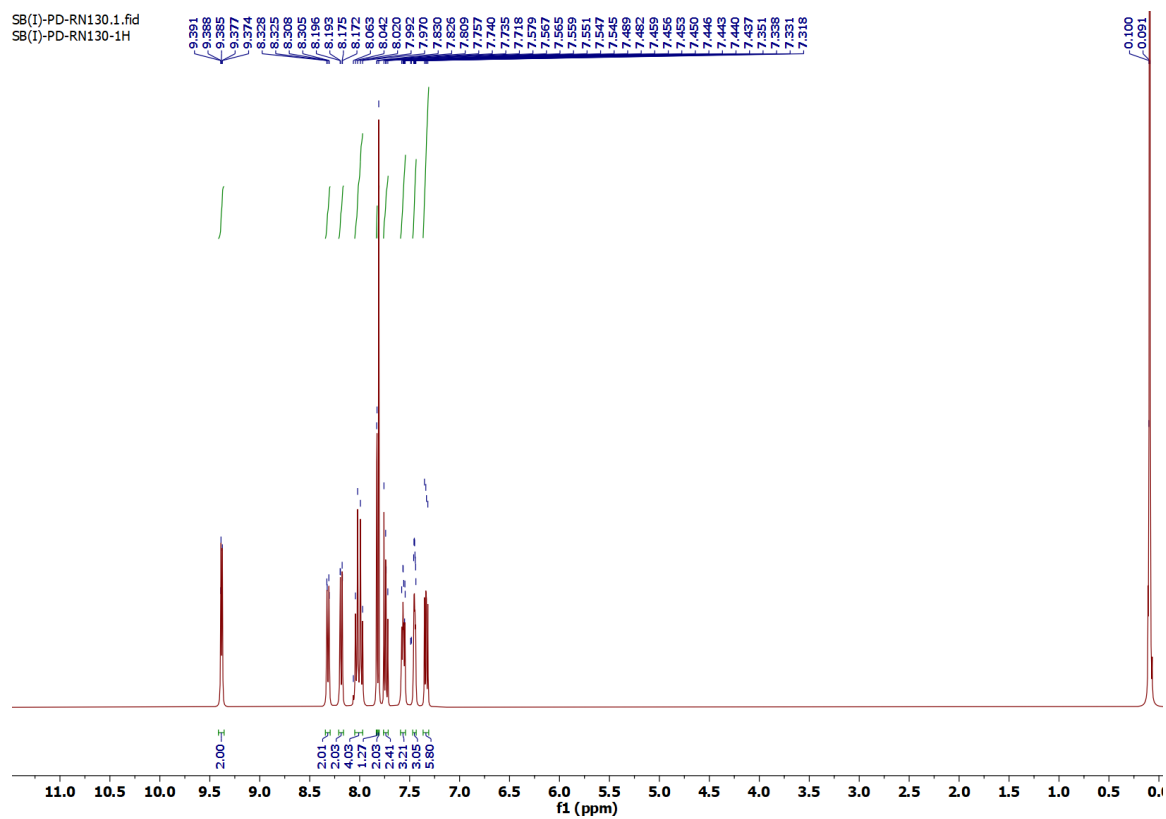


Fig. S16 ^1H NMR spectrum of **4** in CDCl_3 solution.

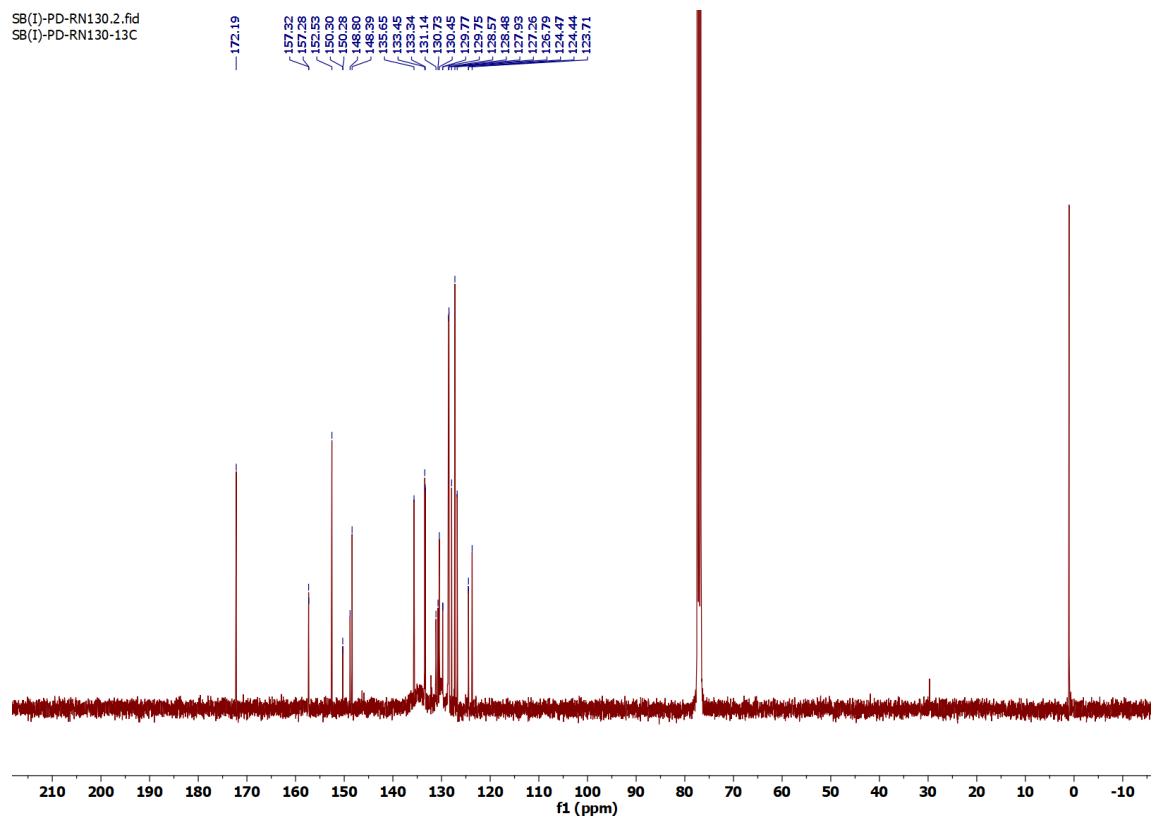


Fig. S17 $^{13}\text{C}\{^1\text{H}\}$ NMR spectrum of **4** in CDCl_3 solution.

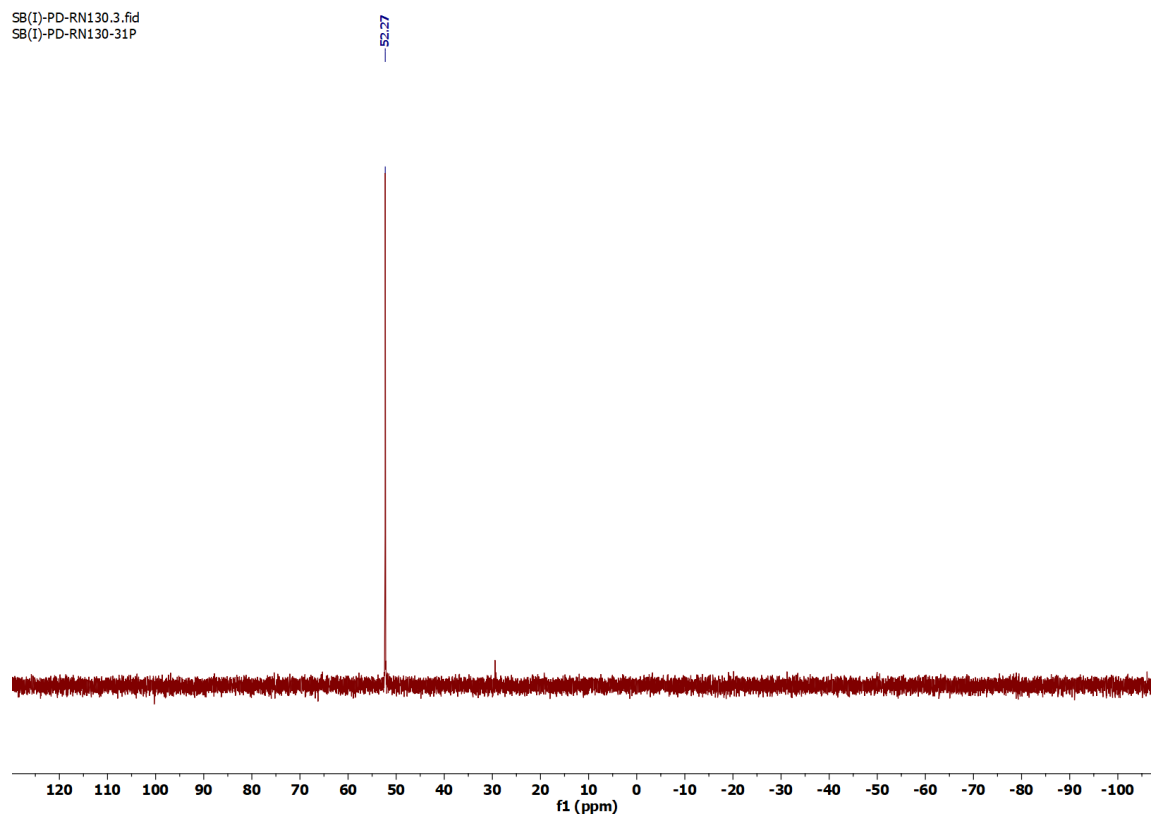


Fig. S18 $^{31}\text{P}\{^1\text{H}\}$ NMR spectrum of **4** in CDCl_3 solution.

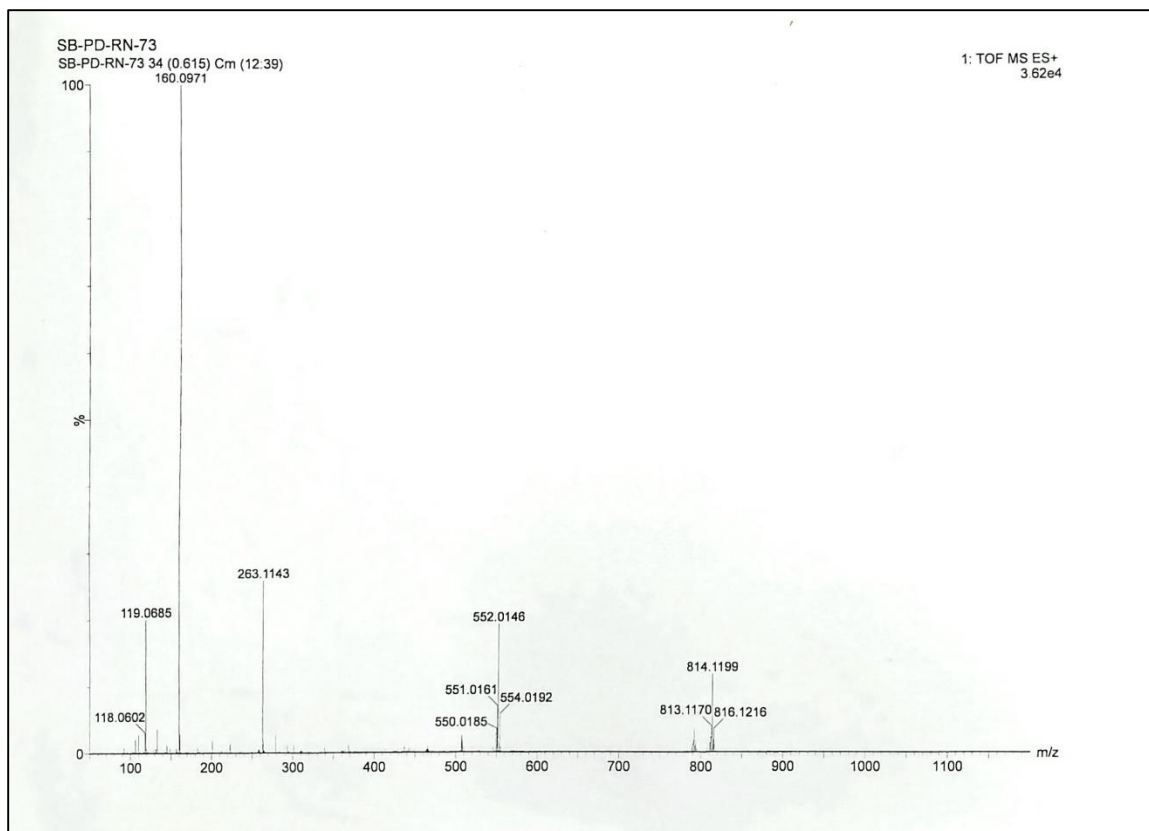


Fig. S19 ESI-MS spectrum of **1**.

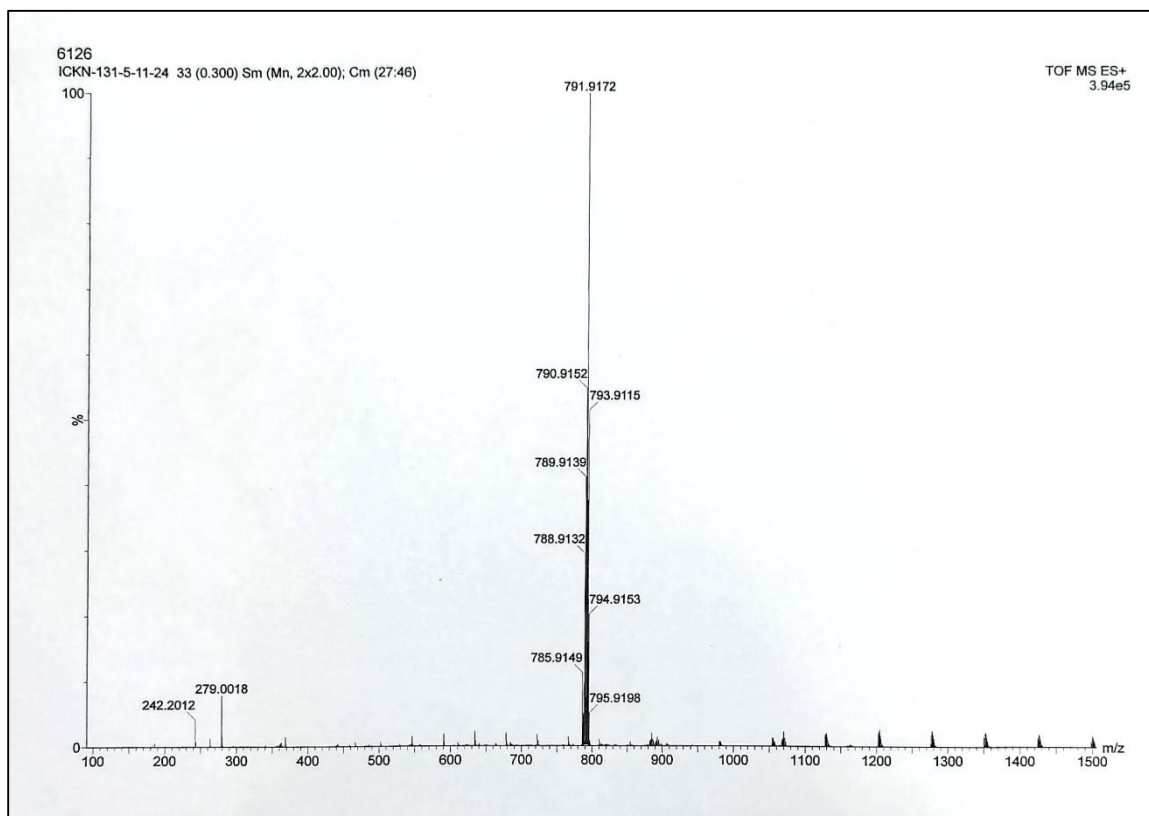


Fig. S20 ESI-MS spectrum of **2**.

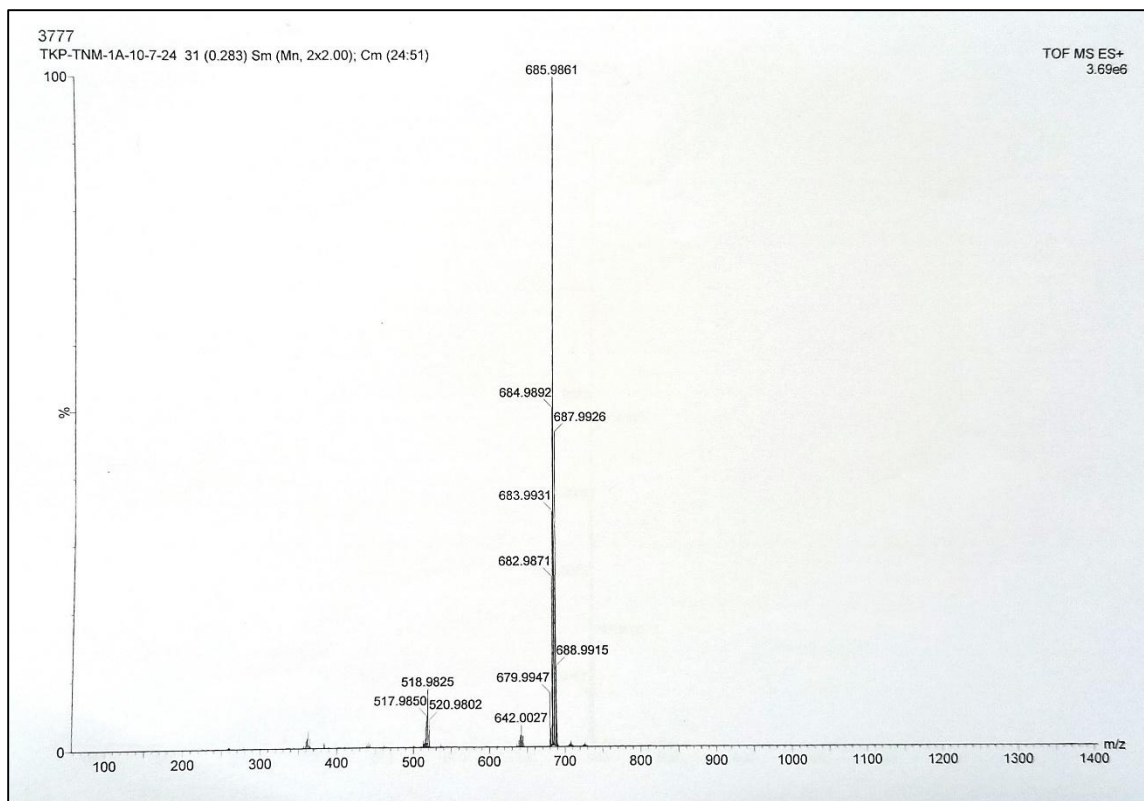


Fig. S21 ESI-MS spectrum of 3.

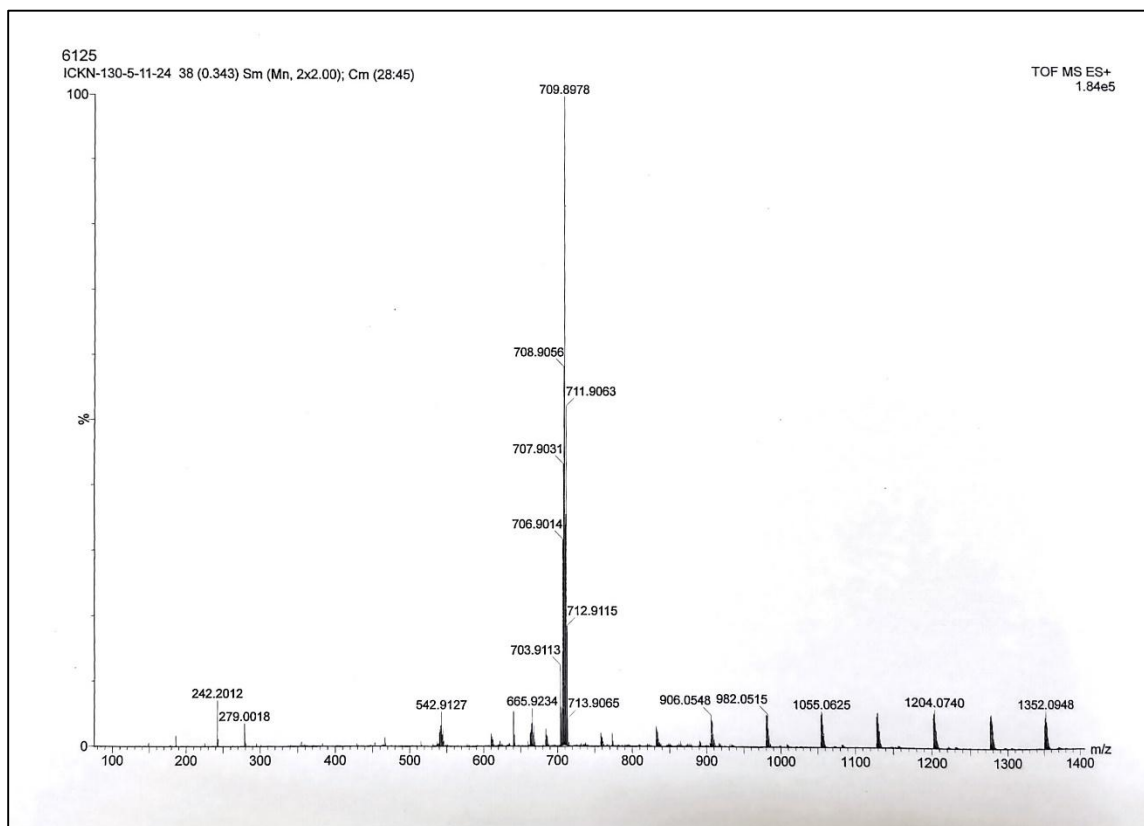


Fig. S22 ESI-MS spectrum of 4.

Table S5 Computed parameters from TDDFT calculations on complex **1** for electronic spectral properties in methanol solution

Excited State	Composition	CI value	E (eV)	Oscillator strength (f)	λ_{theo} (nm)	Assignment	λ_{exp} (nm)
3	H-2 \rightarrow L	0.10167	3.3138	0.0602	374.15	MLCT/LLCT	459
	H-1 \rightarrow L+1	0.69043				MLCT/LLCT	
8	H-2 \rightarrow L	0.66426	3.7094	0.1472	334.24	MLCT/LLCT	361
	H-2 \rightarrow L+2	0.11316				MLCT/LLCT	
	H-2 \rightarrow L+4	0.10065				MLCT/LLCT	
79	H-6 \rightarrow L+2	0.11626	5.3017	0.0730	233.86	LLCT/LMCT	268
	H-4 \rightarrow L+4	0.19772				LLCT/LMCT	
	H-3 \rightarrow L+2	0.20626				LLCT/LMCT	
	H-3 \rightarrow L+4	0.37762				LLCT/LMCT	
	H-3 \rightarrow L+5	0.17837				LLCT/LMCT	
	H-3 \rightarrow L+7	0.14843				LLCT/LMCT	
	H-2 \rightarrow L+10	0.16199				MLCT/LLCT	

Table S6 Compositions of selected molecular orbitals of complex **1** associated with the electronic spectral transitions

% Contribution of fragments to	Fragments				
	Ru	MeCN	PPh ₃ (1)	PPh ₃ (2)	DPA
H-1	64	2	1	2	31
H-2	68	3	8	5	16
H-3	1	0	0	0	99
H-4	4	0	9	1	86
H-6	6	0	76	3	15
LUMO (L)	3	0	3	1	93
L+1	0	0	0	3	97
L+2	9	3	60	26	2
L+4	5	0	62	30	3
L+5	10	4	41	43	2
L+7	3	1	43	51	2
L+10	2	0	88	10	0

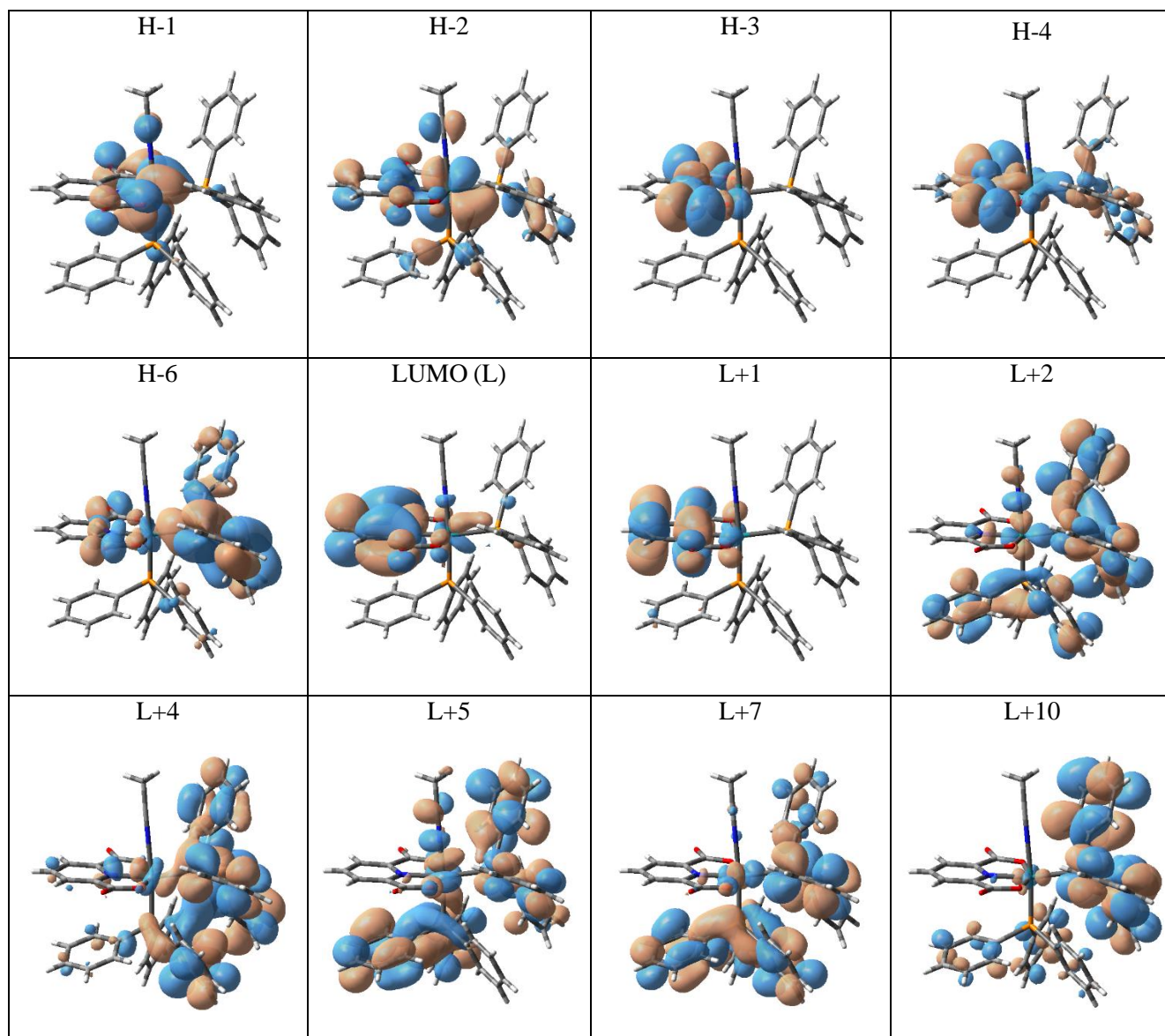


Fig. S23 Contour plots of the molecular orbitals of complex **1**, which are associated with the electronic spectral transitions (See **Table S5**).

Table S7 Computed parameters from TDDFT calculations on complex **2** for electronic spectral properties in acetonitrile solution

Excited State	Composition	CI value	E (eV)	Oscillator strength (f)	λ_{theo} (nm)	Assignment	λ_{exp} (nm)
7	H-2 \rightarrow L	0.67454	3.2923	0.1004	376.59	MLCT/LLCT	454
27	H-10 \rightarrow L	0.12360	4.2813	0.0761	289.59	LLCT/LMCT	362
	H-2 \rightarrow L+2	0.64551				MLCT/LLCT	
98	H-8 \rightarrow L+3	0.19343	5.3289	0.0376	232.66	LLCT/MLCT	262
	H-8 \rightarrow L+4	0.18742				LLCT/MLCT	
	H-7 \rightarrow L+2	0.16610				LLCT	
	H-5 \rightarrow L+3	0.25100				LLCT/MLCT	
	H-5 \rightarrow L+4	0.30057				LLCT/MLCT	
	H-4 \rightarrow L+3	0.21253				LLCT/LMCT	
	H-4 \rightarrow L+4	0.31488				LLCT/LMCT	
	H-4 \rightarrow L+5	0.12434				LLCT/LMCT	
	H-3 \rightarrow L+5	0.10354				LLCT	

Table S8 Compositions of selected molecular orbitals of complex **2** associated with the electronic spectral transitions

% Contribution of fragments to	Fragments				
	Ru	4-picoline	PPh ₃ (1)	PPh ₃ (2)	DPA
H-2	72	3	6	5	14
H-3	2	0	0	0	98
H-4	0	0	35	64	1
H-5	3	3	23	60	11
H-7	2	3	19	54	22
H-8	1	3	41	53	2
H-10	1	5	63	16	15
LUMO (L)	3	1	1	1	94
L+2	2	78	16	2	2
L+3	2	61	31	1	5
L+4	2	0	6	90	2
L+5	2	8	67	22	1

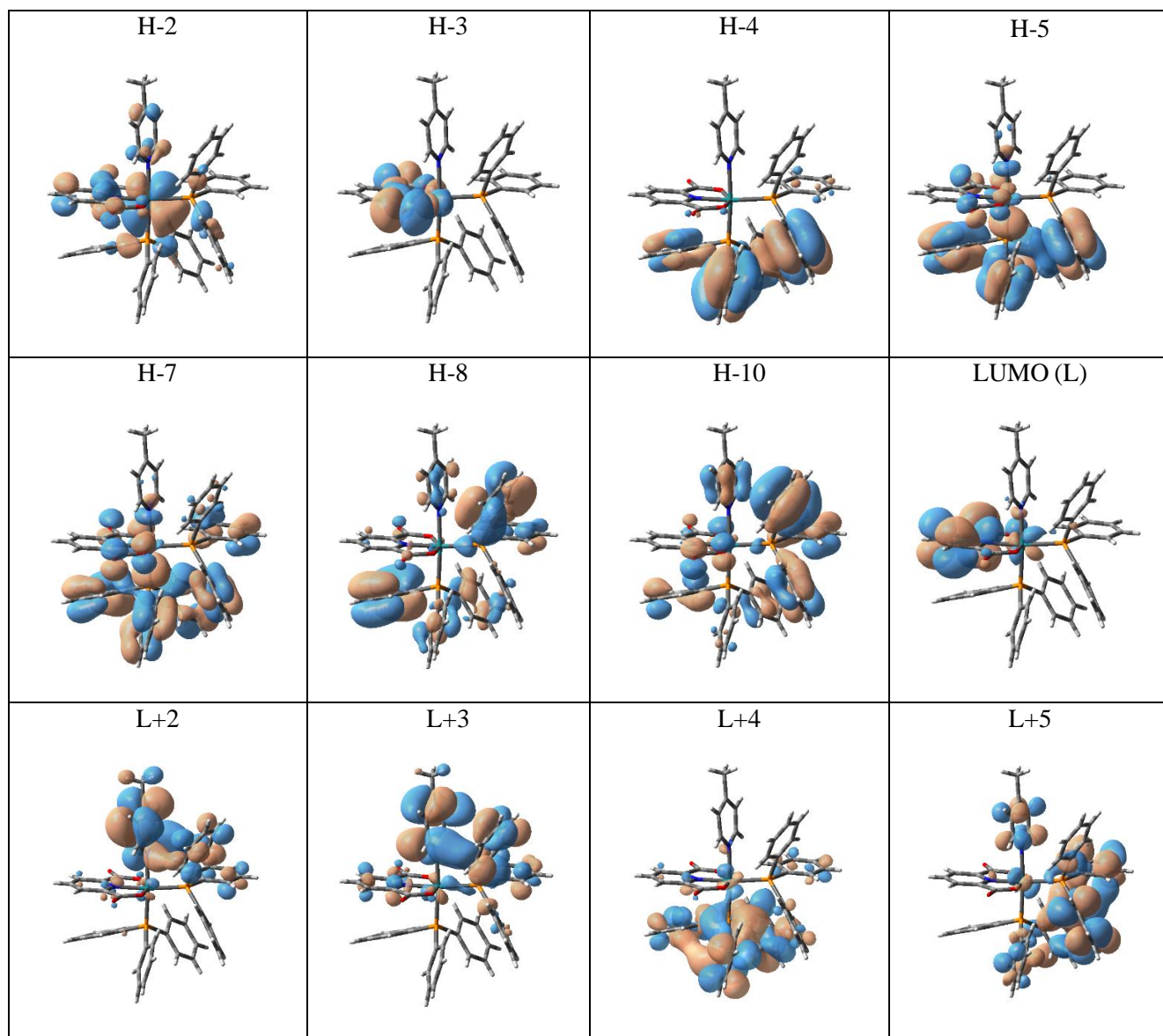


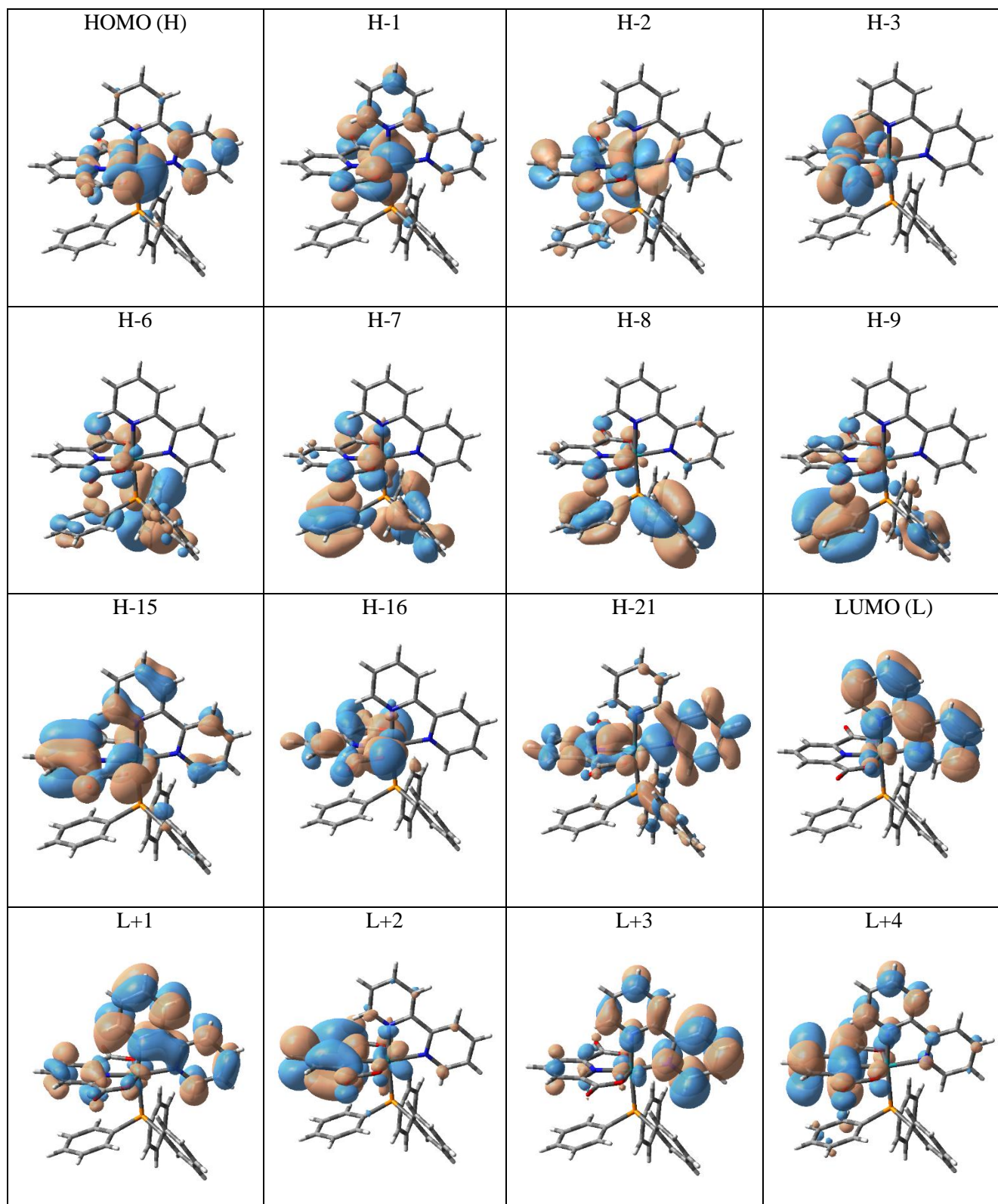
Fig. S24 Contour plots of the molecular orbitals of complex **2**, which are associated with the electronic spectral transitions (See **Table S7**).

Table S9 Computed parameters from TDDFT calculations on complex **3** for electronic spectral properties in acetonitrile solution

Excited State	Composition	CI value	E (eV)	Oscillator strength (f)	λ_{theo} (nm)	Assignment	λ_{exp} (nm)
3	H-1 \rightarrow L	0.63806	2.6069	0.0932	475.60	MLCT/LLCT	513
	H \rightarrow L	0.23872				MLCT/LLCT	
	H \rightarrow L+1	0.11771				MLCT/LLCT	
12	H-2 \rightarrow L+1	0.43887	3.5036	0.1171	353.88	MLCT/LLCT	387
	H-1 \rightarrow L+2	0.10027				MLCT/LLCT	
	H-1 \rightarrow L+3	0.50622				MLCT/LLCT	
36	H-9 \rightarrow L	0.16716	4.4913	0.2624	276.05	LLCT/LMCT	299
	H-7 \rightarrow L	0.62354				LLCT/LMCT	
90	H-21 \rightarrow L	0.10230	5.4056	0.1327	229.36	LLCT/LMCT	263
	H-16 \rightarrow L	0.10434				LLCT/MLCT	
	H-15 \rightarrow L	0.18178				LLCT/MLCT	
	H-8 \rightarrow L+4	0.22810				LLCT/MLCT	
	H-7 \rightarrow L+4	0.24834				LLCT/MLCT	
	H-6 \rightarrow L+5	0.15602				LMCT/LLCT	
	H-3 \rightarrow L+6	0.40871				LLCT/LMCT	

Table S10 Compositions of selected molecular orbitals of complex **3** associated with the electronic spectral transitions

% Contribution of fragments to	Fragments			
	Ru	bpy	PPh ₃	DPA
HOMO (H)	66	10	1	23
H-1	61	7	2	30
H-2	69	3	7	21
H-3	1	0	0	99
H-6	2	0	83	15
H-7	2	1	65	32
H-8	1	1	86	12
H-9	1	0	80	19
H-15	11	11	3	75
H-16	10	1	2	87
H-21	3	53	7	37
LUMO (L)	6	92	1	1
L+1	3	85	1	11
L+2	5	3	2	90
L+3	2	92	1	5
L+4	0	14	3	83
L+5	7	3	87	3
L+6	8	1	89	2



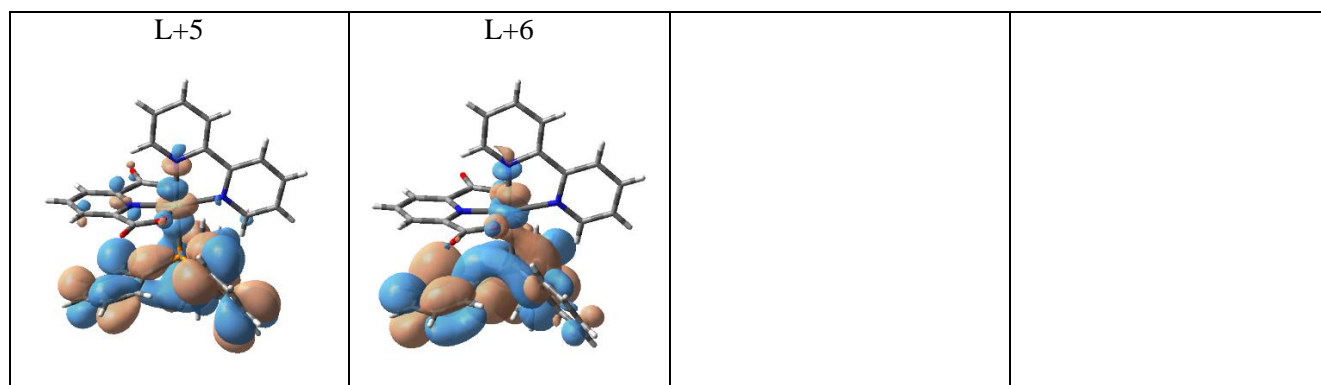


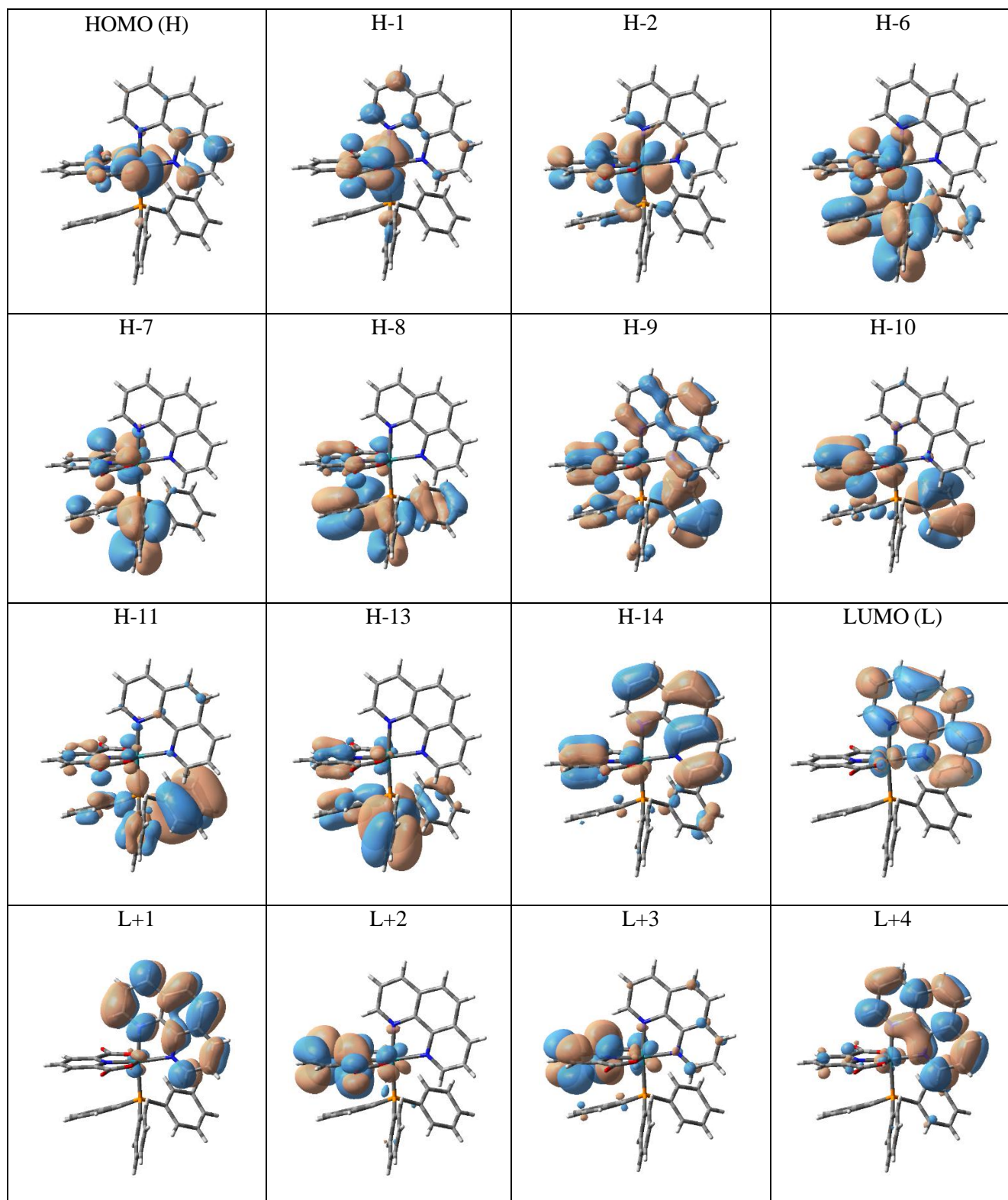
Fig. S25 Contour plots of the molecular orbitals of complex **3**, which are associated with the electronic spectral transitions (See **Table S9**).

Table S11 Computed parameters from TDDFT calculations on complex **4** for electronic spectral properties in acetonitrile solution

Excited State	Composition	CI value	E (eV)	Oscillator strength (f)	λ_{theo} (nm)	Assignment	λ_{exp} (nm)
4	H-1 \rightarrow L	0.51756	2.6570	0.0786	466.62	MLCT/LLCT	476
	H \rightarrow L	0.24878				MLCT/LLCT	
	H \rightarrow L+1	0.20871				MLCT/LLCT	
	H \rightarrow L+2	0.32094				MLCT/LLCT	
15	H-2 \rightarrow L+3	0.56820	3.6675	0.0899	338.06	MLCT/LLCT	386
	H-2 \rightarrow L+4	0.16805				MLCT/LLCT	
	H-2 \rightarrow L+6	0.10052				MLCT/LLCT	
	H \rightarrow L+4	0.11333				MLCT/LLCT	
	H \rightarrow L+5	0.27218				MLCT/LLCT	
69	H-14 \rightarrow L	0.11245	4.8637	0.2272	254.92	LLCT/LMCT	269
	H-13 \rightarrow L+1	0.15110				LLCT/LMCT	
	H-11 \rightarrow L	0.22491				LLCT/LMCT	
	H-11 \rightarrow L+1	0.13565				LLCT/LMCT	
	H-10 \rightarrow L+3	0.10540				LLCT/MLCT	
	H-9 \rightarrow L+1	0.15723				LLCT/MLCT	
	H-8 \rightarrow L+1	0.19173				LLCT/LMCT	
	H-7 \rightarrow L+1	0.14266				LLCT	
	H-7 \rightarrow L+3	0.10250				LLCT/LMCT	
	H-6 \rightarrow L+1	0.12431				LLCT/MLCT	
	H-6 \rightarrow L+3	0.18111				LLCT/MLCT	
	H-1 \rightarrow L+12	0.38372				LLCT/MLCT	
	H-1 \rightarrow L+13	0.12879				LLCT/MLCT	

Table S12 Compositions of selected molecular orbitals of complex **4** associated with the electronic spectral transitions

% Contribution of fragments to	Fragments			
	Ru	phen	PPh ₃	DPA
HOMO (H)	66	10	1	23
H-1	61	7	3	29
H-2	70	3	6	21
H-6	4	2	59	35
H-7	2	1	56	41
H-8	0	0	88	12
H-9	3	18	55	24
H-10	6	2	43	49
H-11	1	3	88	8
H-13	1	0	90	9
H-14	1	69	6	24
LUMO (L)	6	93	0	1
L+1	2	97	0	1
L+2	3	1	3	93
L+3	3	3	2	92
L+4	3	91	3	3
L+5	7	2	88	3
L+6	13	2	82	3
L+12	53	7	22	18
L+13	55	12	25	8



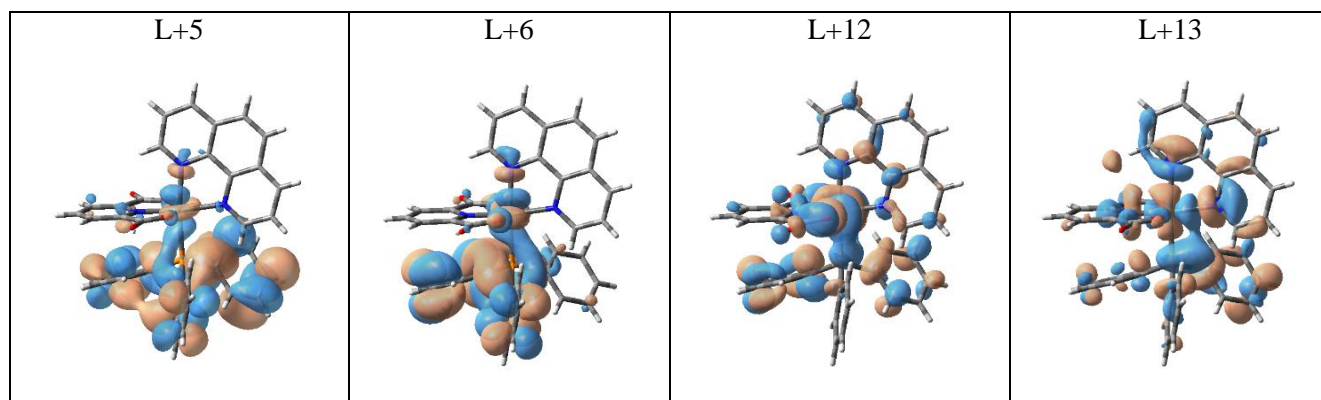
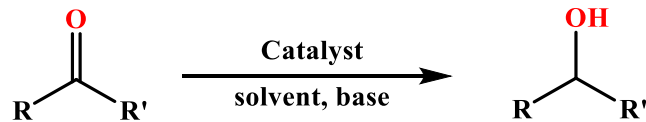
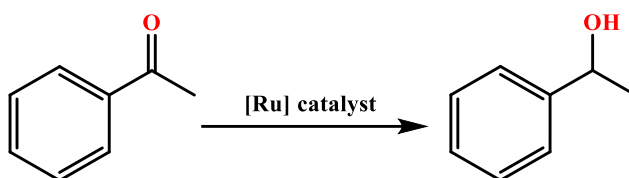


Fig. S26 Contour plots of the molecular orbitals of complex **4**, which are associated with the electronic spectral transitions (See **Table S11**).

Table S13 Optimization of the reaction conditions for the catalysis^a

Entry	Catalyst	Mole % of catalyst	Solvent	Base	Amount of base, equiv.	Temp, °C	Time, h	Yield, %
1	1	1	2-propanol	KOH	1	100	12	NO
2	3	1	2-propanol	KOH	1	100	12	>99
3	3	1	2-propanol	KOH	1	100	6	>99
4	3	1	2-propanol	KOH	1	80	6	48
5	3	0.5	2-propanol	KOH	1	100	6	>99
6	3	0.5	2-propanol	KOH	1	100	3	87
7	3	0.5	2-propanol	KOH	1	100	4	97
8	3	0.5	2-propanol	KOH	1	100	5	>99
9	3	0.5	1-propanol	KOH	1	100	4	68
10	3	0.5	2-propanol	Na ₂ CO ₃	1	100	4	54
11	3	0.5	2-propanol	KO ^t Bu	1	100	4	41
12	3	0.5	2-propanol	KOH	0.1	100	6	39
13	2	0.5	2-propanol	KOH	1	100	4	NO
14	4	0.5	2-propanol	KOH	1	100	4	76
15	-	-	2-propanol	KOH	1	100	4	NO
16	3	0.5	2-propanol	-	-	100	4	NO

^a Reaction conditions: Substrate, Acetophenone (1 mmol); solvent (5.0 mL).

Table S14 Comparison of efficiency of different Ru-catalysts for the transfer hydrogenation

Entry	Cat. loading (mol%)	Time (h)	Yield (%)	TON	TOF (h ⁻¹)	Reference
1	1	24	99	99	4.125	14a
2	2	24	94	47	1.96	14b
3	1	24	99	99	4.125	14c
4	1	24	88.5	88.5	3.68	14d
5	0.7	3	89	127	42	14e
6	1	24	99	99	4.125	14f
7	0.5	1.5	94	188	125	14g
8	1.5	4	99	66	16.5	14h
9	0.1	2	97	970	485	14i
10	0.5	4	97	194	48.5	This work

Table S15 Crystallographic data for complex **1**, **2**, **3** and **4**

Complex	1	2	3	4
Empirical formula	C ₄₅ H ₃₆ N ₂ O ₄ P ₂ Ru	C ₄₉ H ₄₀ N ₂ O ₄ P ₂ Ru, 2[H ₂ O]	C ₃₅ H ₂₆ N ₃ O ₄ PRu, 2[H ₂ O]	2(C ₃₇ H ₂₆ N ₃ O ₄ PRu), 1[CH ₂ CL ₂], 0.9[H ₂ O]
Formula mass	831.81	919.87	720.66	1518.50
Crystal system	Monoclinic	Monoclinic	Monoclinic	Orthorhombic
space group	P2 ₁ /c	P2 ₁ /n	P2 ₁ /n	P2 ₁ 2 ₁ 2 ₁
<i>a</i> (Å)	17.9919(6)	11.009(3)	11.4(3)	11.011 (9)
<i>b</i> (Å)	11.6497(4)	33.411(11)	15.1(4)	16.07(2)
<i>c</i> (Å)	18.6138(6)	11.823(4)	19.2(5)	37.32(4)
<i>α</i> (deg)	90	90	90	90
<i>β</i> (deg)	98.072(2)	90.06	101.3(3)	90
<i>γ</i> (deg)	90	90	90	90
<i>V</i> (Å ³)	3862.8(2)	4349(2)	3262(15)	6605(13)
<i>Z</i>	4	4	4	4
<i>D</i> _{calcd} (g/cm ⁻³)	1.430	1.405	1.467	1.593
<i>F</i> (000)	1701	1896	1472	3208
crystal size (mm ³)	0.08 × 0.11 × 0.16	0.13 × 0.17 × 0.23	0.12 × 0.19 × 0.24	0.14 × 0.16 × 0.32
<i>T</i> (K)	296	252	293	293
<i>μ</i> (mm ⁻¹)	0.535	0.486	0.579	0.702
<i>R</i> 1 ^{<i>a</i>}	0.0276	0.0592	0.0703	0.0847
<i>wR</i> 2 ^{<i>b</i>}	0.0780	0.1627	0.1618	0.2243
GOF ^{<i>c</i>}	1.099	1.026	1.164	1.014

$${}^a R_1 = \sum ||F_o| - |F_c|| / \sum |F_o|$$

$${}^b wR_2 = [\sum [w(F_o^2 - F_c^2)^2] / \sum [w(F_o^2)]]^{1/2}$$

^cGOF = $[\sum [w(F_o^2 - F_c^2)^2] / (M - N)]^{1/2}$, where M is the number of reflections and N is the number of parameters refined.